

Research Paper

# Copper Deportment in a VMS-Hosted Ore from Wetar via Diagnostic Sequential Leaching

Imam Prasetyo<sup>1\*</sup>, Wanidya Ni'immallaili Hadining<sup>1</sup>, Septyo Uji Pratomo<sup>2</sup>, Dhia Ul Faruq Shafarian<sup>1</sup>

<sup>1</sup>Department of Metallurgical Engineering, Universitas Pembangunan Nasional Veteran Yogyakarta, Indonesia

<sup>2</sup>Department of Geological Engineering, Universitas Pembangunan Nasional Veteran Yogyakarta, Indonesia

| Received : September 23, | Revised : September 27, | Accepted : September 30, | Online : October 15, 2025 |
|--------------------------|-------------------------|--------------------------|---------------------------|
| 2025                     | 2025                    | 2025                     |                           |

#### **Abstract**

Copper (Cu) is predominantly sourced from chalcopyrite (CuFeS<sub>2</sub>), which accounts for about 70% of the world's copper reserves. However, chalcopyrite is notoriously refractory to leaching under standard acidic conditions, leading to slow dissolution kinetics and low extraction efficiency. This study investigates the copper deportment in a volcanogenic massive sulfide (VMS)-hosted ore from Wetar Island, Maluku, Indonesia, by employing diagnostic sequential leaching (DSL). The DSL method sequentially leaches the ore with specific reagents to dissolve different copper-bearing mineral fractions. The Wetar ore sample ( $\sim$ 2% Cu) was subjected to a water wash, dilute sulfuric acid leach, and a sodium cyanide leach, sequentially, followed by analysis of the residual solid. Results show that only  $\sim$ 2% of the total copper was water-soluble,  $\sim$ 10% was acid-soluble (as oxides/carbonates), and  $\sim$ 43% was extracted by cyanide (as secondary Cu-sulfides). The largest fraction,  $\sim$ 45%, was left as residual copper. This indicates that while more than half of the copper in this ore exists in easily leachable secondary sulfides and oxides, nearly half remains as refractory primary sulfide (chalcopyrite). These findings inform the design of an optimal extraction strategy, suggesting that conventional leaching could recover a majority of the copper; however, additional measures (e.g., oxidants) would be required to liberate the remaining chalcopyrite-hosted copper.

**Keywords** Chalcopyrite; Diagnostic Sequential Leaching; Copper Deportment; Volcanogenic Massive Sulfide (VMS); Hydrometallurgy

#### INTRODUCTION

Copper is an essential industrial metal with a wide range of applications, and its primary source is chalcopyrite, a copper-iron sulfide mineral (Wang, 2005). Wang (2005) also noted that chalcopyrite-rich porphyry and massive sulfide deposits contain the bulk of global copper reserves. Volcanogenic Massive Sulfide (VMS) deposits are characterized by their heterogeneous mineralogy, which comprises a mixture of primary and secondary copper sulfide minerals. VMS deposits commonly host chalcopyrite as the principal copper mineral, with variable amounts of bornite, chalcocite/digenite, and covellite. In Indonesia, substantial copper resources are found in the eastern islands (e.g., Batu Hijau in Sumbawa and Wetar in Maluku), often as low-grade ores. Traditional processing of copper sulfide ores has relied on pyrometallurgy (smelting), but this approach is economically unfeasible for low-grade ores and poses environmental issues, such as SO<sub>2</sub> emissions (Li et.al., 2018). As an alternative, hydrometallurgical processing, which involves leaching followed by solvent extraction and electrowinning, offers a more sustainable route for low-grade copper ores, with potentially lower emissions and the ability to recover metals selectively

Copyright Holder:

This Article is Licensed Under:



## (Petrović et al., 2023; Tumen-Ulzii et al., 2022).

Despite its advantages, hydrometallurgy faces serious challenges when applied to chalcopyrite. Chalcopyrite does not leach readily in sulfuric acid solutions, exhibiting extremely slow dissolution kinetics and poor copper recovery compared to secondary copper sulfides like chalcocite ( $Cu_2S$ ) or bornite ( $Cu_5FeS_4$ ) (Zou et.al., 2022). This refractory behavior is attributed to inherent mineral properties and leaching phenomena. Firstly, the crystal structure and semiconducting nature of chalcopyrite impede electron transfer at the mineral-solution interface, thereby reducing the reaction rate (Panyushkina et al., 2022). Secondly, chalcopyrite is notoriously sluggish to leach because passive films and coupled kinetic limitations inhibit dissolution, as highlighted by O'Connor and Eksteen (2020) and Nicol et al. (2010). The exact composition of the passive layer is debated, but it often includes iron oxy-hydroxide/sulfate species (e.g., jarosite) and elemental sulfur ( $S^0$ ) or metal-deficient polysulfides (Ghahreman et al., 2020; Yang et al., 2018).

Sutherland (2010) and Nemati et al. (2011) showed that diagnostic (sequential) leaching can partition copper into operational fractions—water-, acid-, cyanide/ammonia-soluble, and residual—serving as practical proxies for mineral associations and liberation without a whole mineralogical campaign. As emphasized by Van Staden and Petersen (2021), such partitioning can guide reagent selection, particle-size targets, and the design of column/heap leaching tests. This work applies a four-step diagnostic leach to a VMS ore and (i) quantifies the balance between readily leachable and refractory copper, (ii) elucidates size-dependent trends that reflect liberation and encapsulation, and (iii) proposes operating windows and additives for column/heap testing.

#### LITERATURE REVIEW

# Mineralogical and Physical Factors in Copper Leaching

The leachability of copper ores is fundamentally governed by their mineralogy. For instance, O'Connor and Eksteen (2020) synthesized mechanisms by which chalcopyrite (CuFeS $_2$ ) becomes refractory via passivation and slow kinetics. In contrast, studies by Yévenes et al. (2010) and Nicol et al. (2010) have shown that other minerals, such as bornite and chalcocite/covellite, tend to dissolve more readily under suitable conditions. Beyond mineralogy, physical characteristics are also critical, with Saldaña et al. (2022) and Van Staden and Petersen (2021) noting that particle size in particular controls both surface area and liberation. However, this relationship is complex; very fine fractions may show higher residual copper due to encapsulation, whereas mid-sized fractions can favor more leachable phases when liberation is adequate.

# Diagnostic Sequential Leaching: The Methodological Framework

Diagnostic sequential leaching is a key method for revealing copper deportment trends that inform flowsheet decisions, as demonstrated by Sutherland (2010) and Nemati et al. (2011). Among the various approaches, a widely used protocol is the acid-cyanide-residual scheme first proposed by Parkison and Bhappu (1995). Proper implementation of such protocols requires careful analytical considerations to ensure data reliability.

## **Leaching Chemistry and Considerations for Scale-Up**

A deep understanding of leaching chemistry is crucial for effectively applying diagnostic results. The choice of lixiviant is critical; for instance, Hedjazi and Monhemius (2018) and Xie et al. (2013) reviewed alternative systems, such as ammoniacal and thiosulfate, that stabilize copper complexes. Even within a single system, the chemistry can be nuanced, as Medina and Anderson (2020) examined the specific implications of cyanide speciation in Cu-bearing ores. Chloridebearing media represent another important approach, where the role of cupric/chloride ions, oxidants, and process variables, such as NaCl concentration, are key factors for success (Torres et

al., 2019; Torres et al., 2020; Skrobian et al., 2005). Ultimately, these chemical insights are crucial when scaling up to processes such as column or heap leaching, which are governed by coupled surface reactions and mass transport (Van Staden & Petersen, 2021; Saldaña et al., 2022). Therefore, the diagnostic results directly inform the selection of reagent strength, Eh-pH targets, and additive strategies for successful large-scale application.

#### **RESEARCH METHOD**

#### **Methods**

The feed is a VMS-hosted sulfide ore from Wetar Island, Maluku, Indonesia. A diagnostic sequential leaching test was employed to evaluate copper solubility under various chemical conditions. The study relied on primary data obtained from laboratory test results. The outcomes include quantification of copper fractions: 1) Water-soluble (WS); 2) Acid-soluble (AS); 3) Cyanide-soluble (CN); and 4) Residual (RES).

The diagnostic leach required fine ores, so the samples had to be prepared. The samples were crushed using a Boyd crusher and then sized using a sieve shaker. The crushed product was separated by particle size, and the diagnostic leach was subsequently carried out for each size fraction. The size fractions obtained were 25; 19; 13.2; 6.7; 3.35; 1.7; 0.85; 0.3; 0.15; 0.106; 0.075; and 0.035 mm. Diagnostic leach analysis was conducted using 100 mL volumetric flasks, 100 mL beakers, Whatman filter paper, a magnetic stirrer, an atomic absorption spectrometer (AAS), and a centrifuge. Calibration standards for sulphuric acid–soluble copper (5 ppm and 20 ppm, or 10 ppm and 30 ppm Cu) were prepared in 2.5%  $\rm H_2SO_4$ ; sodium cyanide–soluble copper standards (5 ppm and 20 ppm, or 10 ppm and 30 ppm Cu) were prepared in 5% HCl.

A 1.0 g sample was weighed into a 50 mL graduated test tube, followed by the addition of 20 mL of distilled water to obtain the water-soluble fraction. The mixture was shaken for 30 minutes at room temperature, then centrifuged for 10 minutes. The supernatant was decanted into a 100 mL volumetric flask. The residue was washed twice with 20 mL of deionized (DI) water for 5 minutes each, then centrifuged, and the washings were combined with the initial extract in the volumetric flask. The combined solution was diluted to the 100 mL mark, stoppered, shaken, and analyzed by AAS using the appropriate calibration standards. For the sulphuric acid–soluble fraction, 20 mL of 10%  $\rm H_2SO_4$  was added to the residue, capped, and shaken for 30 minutes at 20–25°C (±2°C). The mixture was centrifuged for 10 minutes, and the supernatant was decanted into a 100 mL volumetric flask. The residue was washed twice with 20 mL DI water, centrifuged, and the washings combined with the extract. The solution was diluted to volume, mixed, and analysed by AAS.

For the sodium cyanide–soluble fraction, 20 mL of 10% NaCN stock solution was added to the residue from the acid-soluble step, capped, and shaken for 30 minutes at approximately 25 °C. The mixture was centrifuged for 15 minutes, and the supernatant was decanted into a 100 mL Nessler color tube. The residue was washed twice with 20 mL DI water, centrifuged, and the washings combined with the extract. The combined solution was diluted to 200 mL, mixed, and analyzed by AAS. Finally, the residue from the sodium cyanide–soluble step was transferred to a 150 mL beaker with minimal DI water (10–20 mL) and digested with 10 mL HCl, 10 mL HNO $_3$ , and 4 mL perchloric acid to near dryness. Heating the beaker on the hotplate to a temperature of up to 130 °C, until all the acid vaporizes (sample is dry/not burnt). The beaker was removed from the hotplate, cooled to room temperature, and 30–40 mL DI water plus 10 mL HCl were added. The mixture was boiled for 3–5 minutes to dissolve the salts, leaving undigested silicate minerals. After cooling, the solution was diluted to 100 mL with DI water, mixed, and analysed by AAS using the appropriate calibration standards.

## Instrumentation, Data Qualification, and Safety

Copper concentrations were measured by atomic absorption spectroscopy (AAS). As full quality-control documentation (calibration curves, regression coefficients, blanks, duplicates, and drift checks) was not compiled in this research, the reported values should be regarded as indicative. Accordingly, the data are suitable for interpreting copper deportment trends rather than for establishing absolute grade certification. All cyanide-related procedures were conducted under institutional safety protocols, including segregated handling, dedicated protective equipment, and detoxification of effluents. While alkaline conditions (pH > 10) are standard practice to ensure both safety and reagent stability, pH measurements were not recorded during the experiments. Consequently, compliance with optimal cyanide conditions cannot be independently verified for this dataset.

# FINDINGS AND DISCUSSION Result

The experimental data generated in this study are summarized in Tables 1–3. Table 1 presents the weight fraction analysis obtained from the particle size distribution of the crushed ore, including cumulative passing values that were used to calculate the  $P_{80}$ . Table 2 reports the size-by-size metal assays (Cu, Fe, Zn, Al, Mn), which provide the basis for calculating mass-weighted feed grades. Table 3 summarizes the results of the copper soluble analysis from the sequential diagnostic leaching tests, showing the distribution of copper into water-soluble, acid-soluble, cyanide-soluble, and residual fractions for each size class. Together, these datasets establish the quantitative framework for evaluating copper deportment in the studied VMS ore.

Table 1. Weight Fraction Analysis

| Size     | Retained | Retained   | Cumulative     | Cumulative     | P80 Size |
|----------|----------|------------|----------------|----------------|----------|
| Fraction | Weight   | Percentage | Passing        | Retained       |          |
| (mm)     | (gram)   | (%)        | Percentage (%) | Percentage (%) | (mm)     |
| 25       | 1.25     | 0.17       | 0.83           | 1.00           |          |
| 19       | 1.85     | 0.26       | 0.57           | 0.83           | 24.27    |
| 13.2     | 1.6      | 0.22       | 0.35           | 0.57           |          |
| 6.7      | 0.965    | 0.13       | 0.22           | 0.35           |          |
| 3.35     | 0.425    | 0.06       | 0.16           | 0.22           |          |
| 1.7      | 0.275    | 0.04       | 0.12           | 0.16           |          |
| 0.85     | 0.215    | 0.03       | 0.09           | 0.12           |          |
| 0.3      | 0.26     | 0.04       | 0.06           | 0.09           |          |
| 0.15     | 0.16     | 0.02       | 0.03           | 0.06           |          |
| 0.106    | 0.065    | 0.01       | 0.02           | 0.03           |          |
| 0.075    | 0.095    | 0.01       | 0.01           | 0.02           |          |
| 0.035    | 0.085    | 0.01       | 0.00           | 0.01           |          |
| Total    | 7.245    | 1.00       | 0.83           | 1.00           | 24.27    |

Table 2. Metal Assay

| Size Fraction (mm) | Copper<br>Grade<br>(%) | Iron Grade<br>(%) | Zinc Grade<br>(%) | Aluminium<br>Grade (%) | Manganese<br>Grade (%) |
|--------------------|------------------------|-------------------|-------------------|------------------------|------------------------|
| 25                 | 1.46                   | 40.8              | 0.42              | 0.01                   | 0.02                   |
| 19                 | 1.69                   | 41.3              | 0.58              | 0.01                   | 0.02                   |

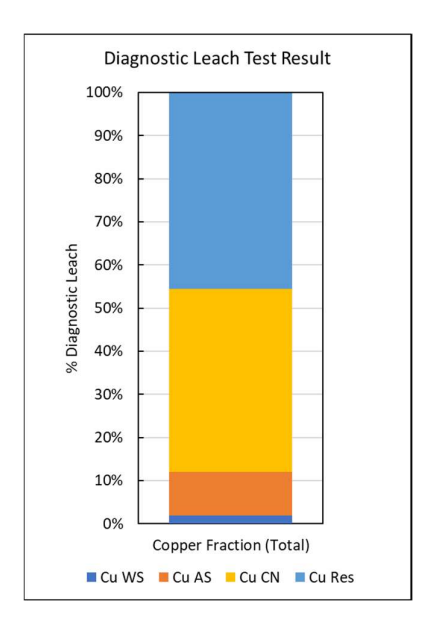
| Size Fraction (mm) | Copper<br>Grade<br>(%) | Iron Grade<br>(%) | Zinc Grade<br>(%) | Aluminium<br>Grade (%) | Manganese<br>Grade (%) |
|--------------------|------------------------|-------------------|-------------------|------------------------|------------------------|
| 13.2               | 1.38                   | 41.7              | 0.71              | 0.01                   | 0.03                   |
| 6.7                | 2.09                   | 36.3              | 1.03              | 0.01                   | 0.02                   |
| 3.35               | 2.65                   | 35.5              | 1.2               | 0.01                   | 0.02                   |
| 1.7                | 2.73                   | 36.2              | 1.43              | 0.02                   | 0.13                   |
| 0.85               | 2.83                   | 35.4              | 1.51              | 0.01                   | 0.36                   |
| 0.3                | 3.42                   | 33.7              | 1.68              | 0.05                   | 0.02                   |
| 0.15               | 3.74                   | 29.5              | 1.7               | 0.11                   | 0.01                   |
| 0.106              | 4.35                   | 25.3              | 1.87              | 0.17                   | 0.01                   |
| 0.075              | 4.99                   | 23.7              | 2.04              | 0.2                    | 0.02                   |
| 0.04               | 5.83                   | 22.30             | 2.28              | 0.01                   | <0.01                  |
| Total              | 1.99                   | 38.80             | 0.85              | 0.02                   | 0.04                   |

**Table 3.** Copper Soluble Analysis

| Size Fraction | Cu WS  | Cu AS   | Cu CN   | Cu Res  |
|---------------|--------|---------|---------|---------|
| (mm)          | (mg/l) | (mg/l)  | (mg/l)  | (mg/l)  |
| 25            | 106    | 1378    | 7170    | 6256    |
| 19            | 249    | 1452    | 6580    | 8690    |
| 13.2          | 130    | 1281    | 5640    | 6700    |
| 6.7           | 303    | 2578    | 9230    | 7701    |
| 3.35          | 282    | 2749    | 10930   | 10480   |
| 1.7           | 145    | 3402    | 11620   | 11120   |
| 0.85          | 497    | 3594    | 13240   | 12270   |
| 0.3           | 762    | 4091    | 15020   | 13780   |
| 0.15          | 1362   | 3754    | 12370   | 20030   |
| 0.106         | 495    | 6118    | 16150   | 18720   |
| 0.075         | 2306   | 4910    | 16970   | 24700   |
| 0.035         | 6824   | 1466    | 23160   | 25100   |
| Total         | 359.90 | 1998.02 | 8318.66 | 8927.87 |

#### **Discussion**

The first diagnostic leach test illustrates the distribution of copper fractions based on total leaching response. Water-soluble copper (Cu WS) accounts for approximately 2% of the total copper, indicating that only a minor portion exists in readily soluble forms such as copper sulfate or oxidized species. Acid-soluble copper (Cu AS) comprises around 10%, suggesting the presence of secondary copper minerals like carbonates (e.g., malachite, azurite) or oxides that are moderately soluble in acid. Cyanide-soluble copper (Cu CN) represents the largest fraction, approximately 43%, typically associated with primary to tertiary copper sulfide minerals such as chalcocite and covellite, which are amenable to dissolution in cyanide/ammonia-based solutions. Residual copper (Cu Res) constitutes about 45%, indicating that nearly half of the copper content is locked within refractory minerals such as primary chalcopyrite, bornite, or silicate-hosted copper



phases. This proportion composition can be seen in Figure 1.

Figure 1. The Overall Copper Deportment

The second diagnostic leach test compares the copper fraction distribution across particle size ranges (from 25 mm to 0.035 mm). A more detailed analysis of each size fraction reveals interesting trends, as illustrated in Figure 2. Water-soluble copper remains consistently low across all size fractions, with a slight increase in finer particles ( $\leq$ 0.075 mm), likely due to higher surface area or the presence of surface-coated secondary copper minerals. Acid-soluble copper ranges between 10–15% across all size classes, indicating a relatively uniform distribution of acid-soluble phases such as oxides and carbonates, independent of particle size.

Cyanide-soluble copper dominates most size fractions, particularly in the mid-size range (6.7--0.85~mm), where it can exceed 60%. In contrast, its proportion decreases in the finest fraction (<0.075 mm), possibly due to a shift toward residual copper, as finer particles expose more primary chalcopyrite that resists conventional leaching. Residual copper contributes significantly across all size fractions, especially in coarse (25–19 mm) and ultra-fine (<0.075 mm) particles. In coarse fractions, this may be attributed to mineral encapsulation or incomplete liberation, while in fine fractions, the high Cu Res content reflects the dominance of refractory chalcopyrite.

The findings from this study provide several important implications for the design of a hydrometallurgical process for this ore. Given the dominance of the CN-soluble fraction, the application of a leach system using a complexing agent, such as cyanidation or ammonia leaching, is highly recommended. However, to target the significant residual fraction, a more aggressive approach is required. In line with previous studies by O'Connor and Eksteen (2020), we prioritize oxidizing conditions for chalcopyrite-rich feeds. Torres et al. (2019) and Torres et al. (2020) further support the use of low-to-moderate chloride and  $MnO_2$  as kinetic enhancers, while Skrobian et al. (2005) quantified the effects of NaCl concentration and particle size on dissolution. Therefore, as a next step, a series of column leach tests is highly recommended to systematically evaluate the combined effects of a complexing agent, Eh control, and chloride addition.

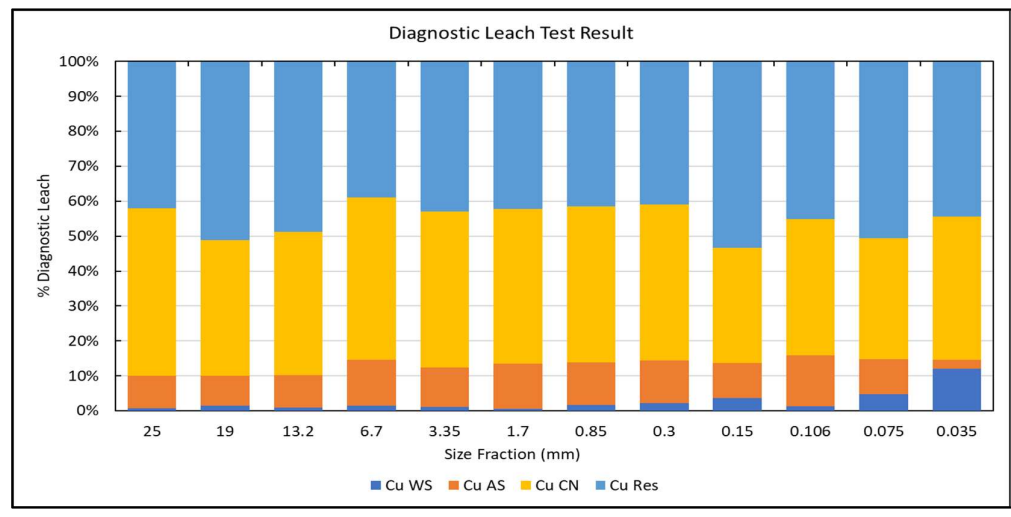


Figure 2. Copper Deportment by Size Fraction (Operational Fractions)

It is important to note the limitations of this study. The classification of copper fractions is operational and does not provide definitive mineralogical identification. Although the residual fraction is very likely dominated by chalcopyrite, further confirmation is needed. Therefore, these results should be used as a strong preliminary guide to be verified by quantitative mineralogical analysis (such as QEMSCAN or XRD-Rietveld) and through the recommended further leach testing.

#### **CONCLUSIONS**

This study demonstrates that the four-step diagnostic leach (WS-AS-CN-RES) effectively maps copper deportment in the studied VMS ore from Wetar Island, Maluku, Indonesia. The results reveal that the sample is dominated by a cyanide-soluble copper fraction ( $\sim$ 43%) but also contains a substantial residual fraction ( $\sim$ 45%), suggesting a mix of readily leachable phases and refractory chalcopyrite. This conclusion is further supported by size effects, which show increasing residual copper at particle sizes  $\leq$ 0.15 mm, a finding consistent with the dominance of refractory chalcopyrite in the fines. Based on these findings, future research should prioritize methods to extract the significant residual fraction. Therefore, future column tests should prioritize oxidizing conditions, the optional addition of MnO<sub>2</sub>, and low-to-moderate NaCl concentrations to accelerate extraction from the refractory sulphide phases. It should be noted that the classification of copper fractions in this study is operational and requires further verification through quantitative mineralogical analysis (such as QEMSCAN or XRD-Rietveld) for definitive confirmation.

# REFERENCES

Ghahreman, A., Wang, J., & Faraji, F. (2020). Effect of ultrasound on the oxidative copper leaching from chalcopyrite in acidic ferric sulfate media. *Minerals*, 10(7), 1–17. https://doi.org/10.3390/min10070633

Hedjazi, F., & Monhemius, A. J. (2018). Industrial application of ammonia-assisted cyanide leaching for copper-gold ores. *Minerals Engineering*, *126*, 123-129. https://doi.org/10.1016/j.mineng.2018.07.005

Heltai, G., Győri, Z., Fekete, I., Halász, G., Kovács, K., Takács, A., ... & Horváth, M. (2019). Application of flexible multi-elemental ICP-OES detection in fractionation of potentially toxic element content of solid environmental samples by a sequential extraction procedure. *Microchemical Journal*, 149, 104029. https://doi.org/10.1016/j.microc.2019.104029.

- Medina, D., & Anderson, C. G. (2020). A review of the cyanidation treatment of copper-gold ores and concentrates. *Metals*, 10(7), 897. https://doi.org/10.3390/met10070897
- Nemati, K., Bakar, N. K. A., Bin Abas, M. R., Sobhanzadeh, E., & Low, K. H. (2011). Comparison of unmodified and modified BCR sequential extraction schemes for the fractionation of heavy metals in shrimp aquaculture sludge from Selangor, Malaysia. *Environmental monitoring and assessment*, 176(1), 313-320. https://doi.org/10.1007/s10661-010-1584-3
- Nicol, M. J., Miki, H., & Velásquez-Yévenes, L. V. (2010). The dissolution of chalcopyrite in chloride solutions: Part 3. Mechanisms. *Hydrometallurgy*, 103(1–4), 86–95. https://doi.org/10.1016/j.hydromet.2010.03.003
- O'Connor, G. M., & Eksteen, J. J. (2020). A critical review of the passivation and semiconductor mechanisms of chalcopyrite leaching. *Minerals Engineering*, 154, 106401. https://doi.org/10.1016/j.mineng.2020.106401
- Panyushkina, A. E., Fomchenko, N. V., & Muravyov, M. I. (2022). Comparison of Bio-and Ferric Leaching for Beneficiation of Bulk Copper-Nickel Sulfidic Concentrate. *IOP Conference Series: Earth and Environmental Science, 1046*(1). https://doi.org/10.1088/1755-1315/1046/1/012005
- Parkison, G. A., & Bhappu, R. B. (1995). *The Sequential Copper Analysis Method–Geological, Mineralogical, And Metallurgical Implications*. SME Preprint No. 95–90, Littleton, CO, USA.
- Petrović, S. J., Bogdanović, G. D., Antonijević, M. M., Vukčević, M., & Kovačević, R. (2023). The Extraction of Copper from Chalcopyrite Concentrate with Hydrogen Peroxide in Sulfuric Acid Solution. *Metals*, *13*(11), 1818. https://doi.org/10.3390/met13111818
- Saldaña, M., Gálvez, E., Robles, P., Castillo, J., & Toro, N. (2022). Copper mineral leaching mathematical models—A review. *Materials*, 15(5), 1757. https://doi.org/10.3390/ma15051757
- Skrobian, M., Havlik, T., & Ukasik, M. (2005). Effect of NaCl concentration and particle size on chalcopyrite leaching in cupric chloride solution. *Hydrometallurgy*, 77(1-2), 109-114. https://doi.org/10.1016/j.hydromet.2004.10.015
- Sutherland, R. A. (2010). BCR®-701: A review of 10-years of sequential extraction analyses. *Analytica Chimica Acta*, 680(1-2), 10-20. https://doi.org/10.1016/j.aca.2010.09.016
- Torres, C. M., Ghorbani, Y., Hernández, P. C., Justel, F. J., Aravena, M. I., & Herreros, O. O. (2019). Cupric and chloride ions: Leaching of chalcopyrite concentrate with low chloride concentration media. *Minerals*, 9(10), 639. https://doi.org/10.3390/min9100639
- Torres, D., Ayala, L., Jeldres, R. I., Cerecedo-Sáenz, E., Salinas-Rodríguez, E., Robles, P., & Toro, N. (2020). Leaching chalcopyrite with high MnO2 and chloride concentrations. *Metals*, *10*(1), 107. https://doi.org/10.3390/met10010107
- Tumen-Ulzii, N., Garnaad, A., Silam, A., Tumendelger, A., Gunchin, B., Shirchinnamjil, N., Haga, K., Shibayama, A., & Batnasan, A. (2022). Copper Recovery from Chalcopyrite Concentrate by Oxidative Roasting and Acid Leaching. *International Journal of the Society of Material Engineering for Resources*, 25(1), 56–62. https://doi.org/10.5188/IJSMER.25.56
- Van Staden, P. J., & Petersen, J. (2021). Towards fundamentally based heap leaching scale-up. *Minerals Engineering*, 168, 106915. https://doi.org/10.1016/j.mineng.2021.106915
- Wang, S. (2005). Copper leaching from chalcopyrite concentrates. *Jom*, *57*(7), 48-51. https://doi.org/10.1007/s11837-005-0252-5
- Xie, F., Dreisinger, D., & Doyle, F. (2013). A review on recovery of copper and cyanide from waste cyanide solutions. *Mineral Processing and Extractive Metallurgy Review*, 34(6), 387-411. https://doi.org/10.1080/08827508.2012.695303
- Yang, I., Choi, S., & Park, J. (2018). Passivation of chalcopyrite in hydrodynamic-bioleaching. *Episodes*, 41(4), 249–258. https://doi.org/10.18814/epiiugs/2018/018018

Yévenes, L. V., Miki, H., & Nicol, M. (2010). The dissolution of chalcopyrite in chloride solutions: Part 2. Effect of various parameters on the rate. *Hydrometallurgy*, *103*(1-4), 80-85. https://doi.org/10.1016/j.hydromet.2010.03.004

Zou, X., Zhang, Y., Zhou, S., Wang, Z., & Wei, B. (2022). Research progress in intensified bioleaching of chalcopyrite: A review. 4th International Conference on Material Science, Environment Science and Computer Science (MSESCS 2022), 17, 204–211. https://doi.org/10.54097/hset.v17i.2599